ELSEVIER

Journal of Hydrology 255 (2002) 151–168

Journal of Hydrology

www.elsevier.com/locate/jhydrol

Construction of geostatistical aquifer models integrating dynamic flow and tracer data using inverse technique

X.-H. Wen[a,*], C.V. Deutsch[b], A.S. Cullick[c]

[a]*Chevron Petroleum Technology Company, San Ramon, CA, USA*
[b]*Department of Civil and Environmental Engineering, University of Alberta, Edmonton, Alb., Canada*
[c]*Landmark Graphics, Austin, TX, USA*

Received 20 June 2001; revised 27 June 2001; accepted 5 September 2001

Abstract

Natural aquifers are heterogeneous, and geostatistical methods are widely used to simulate the heterogeneity of aquifer properties. Due to limited available data, it is essential to integrate as much information as possible to reduce the uncertainty in aquifer models and flow predictions. Traditional geostatistical techniques efficiently consider static hard and soft information, such as core data and seismic data. However, dynamic flow and transport data, such as flow rates, pressure, and tracer breakthrough, are important information that are not easily considered with the traditional techniques. Integrating such dynamic data into a model requires the solution of a difficult inverse problem, since dynamic data and aquifer properties are related to each other through the non-linear flow and transport equations.

A recently developed geostatistically based inverse technique, the sequential self-calibration (SSC) method, is introduced to integrate those dynamic data. The SSC method is an iterative inverse technique that is coupled with an optimization procedure. It provides for fast generation of multiple realizations of aquifer property models that jointly match pressure and tracer breakthrough data, yet display the same geostatistical characteristics. This method is flexible, computationally efficient, and robust. The main features of SSC include (1) a *master point* concept that reduces the number of parameters, (2) a perturbation mechanism based on kriging that accounts for the spatial correlation of the aquifer properties, (3) a fast streamline-based tracer flow simulator for integration of tracer data, and (4) a new semi-analytical streamline-based method for computing sensitivity coefficients of tracer breakthrough.

Applications of the SSC method are demonstrated with a synthetic data set. Results show that tracer breakthrough data carry important information on the spatial variation of aquifer permeability in the inter-well areas. As a contrast, pressure data provide information at near well-bore areas only. Integrating pressure and breakthrough data jointly leads to significant improvement in the aquifer heterogeneity representation and a reduction in the uncertainty of aquifer model. The accuracy of flow and transport predictions can be dramatically improved by integrating dynamic data.

Keywords: Heterogeneity; Permeability; Dynamic data integration; Tracer breakthrough; Sequential self-calibration method; Streamline simulation

1. Introduction

Optimal management of an aquifer requires reliable flow and transport simulations and forecasts with as little uncertainty as possible. Incomplete data and

* Corresponding author. Fax: +1-925-842-6283.
E-mail address: xwen@chevron.com (X.-H. Wen).

0022-1694/02/$ - see front matter
PII: S0022-1694(01)00512-1

inability to model the physics of fluid flow at a suitably small-scale lead to unavoidable uncertainty. Uncertainties in the detailed description of aquifer lithofacies, porosity, and permeability are large contributors to the uncertainty in flow and transport forecasting. Reducing this uncertainty can only be achieved by integrating additional data in aquifer modeling.

Geostatistical models are widely used to describe the spatial heterogeneity of aquifer properties. A large variety of geostatistical techniques have been developed that can be used to construct aquifer models conditioned to diverse types of static data including hard well data and soft seismic data (e.g. Deutsch and Journel, 1998). Commonly, several techniques are applied hierarchically to model large-scale aquifer geometry, lithofacies, and flow properties such as porosity and permeability. Integration of soft (or secondary) data is usually achieved through a statistical correlation with the hard (or primary) data. Conventional geostatistical techniques including Gaussian, indicator, annealing-based, or object-based methods are not suited to directly integrate dynamic flow and transport data.

Dynamic flow and transport data and aquifer flow properties are related to each other through the highly non-linear flow and transport equations. As a consequence, accounting for dynamic flow and transport data in geostatistical modeling requires the solution of an inverse problem (e.g. Yeh, 1986; Tarantola, 1987; Sun, 1994; Gomez-Hernandez et al., 1997). Although difficult to consider in aquifer modeling, flow and transport data, such as flow rate, flow pressure (or piezometric head), tracer breakthrough curve, and tracer concentration data are often the most important information because they provide direct measurements of the actual aquifer flow character. These dynamic data are closely related to what we want to predict for aquifer management decisions. Integrating such dynamic data is an important outstanding problem in aquifer characterization.

The tedious trial and error methods are widely used in practice because of limitations of automatic methods. Automatic integration of dynamic data in aquifer modeling is an active area of research and a number of inverse techniques have been reported in the literature. Wen et al. (1997) have presented a review of the available methods. Early approaches were based on parameter identification or history matching. The practical usefulness of these methods is limited due to the significant assumptions and intensive computational requirements.

The inverse problem is often ill-posed (small variation in dynamic data may result in unbounded changes in the model estimates) and the solution of the problem is non-unique (more than one solutions can satisfy the same set of dynamic data). Traditional inverse techniques usually seek a single 'best' estimation of aquifer property that best matches the measured dynamic data. This best estimate is usually over-smoothed compared to the spatial variability observed and does not capture the uncertainty inherent in the inverse problem.

In this paper, we present an extension of the sequential self-calibration (SSC) method to generate multiple, equally probable realizations of aquifer permeability models, all of which display the correct degree of spatial variation and match the measured dynamic data. Similar published work includes Carrera and Neuman (1986), Harvey and Gorelick (1995), RamaRao et al. (1995), Zimmerman et al. (1995), Kitanidis (1996), and Yeh et al. (1996). These methods share one or more of the following limitations: (1) results over-smoothed, (2) computationally intensive, (3) only pressure data are used, and (4) only for Gaussian random fields.

In the following sections, we first describe briefly the process of the SSC method. A fast streamline-based semi-analytical method is then presented for fast computation of sensitivity coefficients required for the SSC inversion. A synthetic example is used to demonstrate the efficiency and robustness of the SSC method, followed by a summary.

2. The sequential self-calibration method

The integration of dynamic data in aquifer models can significantly improve the accuracy of aquifer flow and transport predictions. Dynamic data integration in geostatistical aquifer modeling is usually performed through an inverse technique because they are non-linearly related to aquifer properties through the flow and transport equations. The SSC method is an inverse technique originally developed by Gomez-Hernandez and coworkers at Technical University of Valencia,

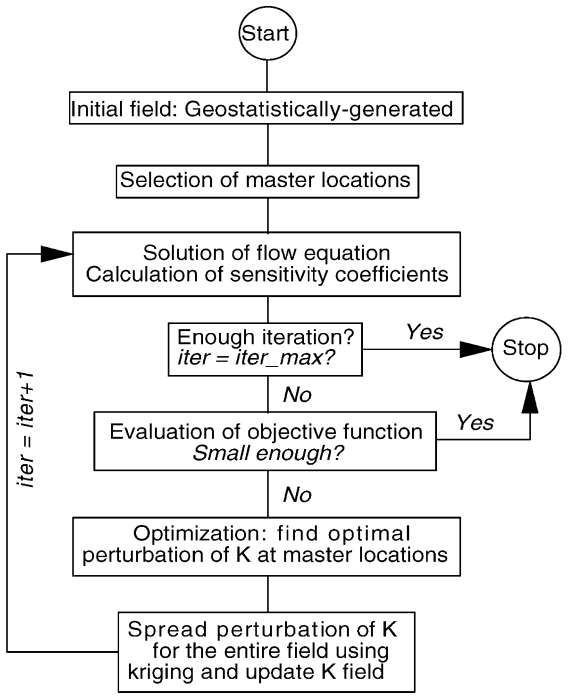

Fig. 1. Flowchart of the SSC method.

Spain (Gomez-Hernandez et al., 1997). The unique features of the SSC algorithm are (1) the concept of *master point* that reduces the parameter space to be estimated in the optimization, (2) the propagation procedure through *kriging* that accounts for spatial correlation of perturbations, and (3) the fast computation of sensitivity coefficients within a single flow simulation run that makes inversion feasible. In this paper, the original SSC method is extended to integrate transient pressure and tracer transport data. The main steps of the SSC method can be summarized as follows.

Construct initial aquifer property realizations by conventional geostatistical methods using a histogram and a variogram that are consistent with the data. If static (hard and soft) data are available, they are honored with conditional simulation. Any geostatistical methods appropriate to the given geology and data set can be used in this step. Each realization is then processed one at a time with the following steps (see Fig. 1):

1. Solve the flow and transport equations for the current model using the specified boundary conditions to obtain the simulation responses.
2. Compute an objective function that measures the mismatch of observed flow and transport data and simulated model responses. If the objective function is smaller than a preselected tolerance, this realization is considered to honor the dynamic data and we move to the next realization. Otherwise, proceed to the next step.
3. Select a few master locations (usually 1–3 per correlation range in each direction) and solve an optimization problem to find the optimal perturbations of aquifer property at these locations. Sensitivity coefficients needed for the optimization are computed while solving the flow and transport equations (step 1). Details of computing sensitivity coefficients are given later.
4. Propagate the perturbations at master locations through the entire model by kriging the computed perturbations at the master points to all grid cells. The model is then globally updated by adding the smooth kriged perturbation field to the current model.
5. Loop back to step 1 until convergence.

Typically, less than 20 iterations are required in a 2D setting. More details on the SSC algorithm and other implementation issues can be found in Wen (1996), Gomez-Hernandez et al. (1997) and Wen et al. (1998a,b, 1999). Typically, tens to hundreds of realizations are constructed. Fewer realizations may be considered if they lead to nearly the same predicted responses.

Application of the SSC method requires a variogram model for the construction of the initial realizations and for kriging the perturbations from the master points to the entire model. The resulting multiple, equally probable realizations of reservoir models provide a means to assess uncertainty of the aquifer model, which can be translated into uncertainty of the flow and transport predictions for aquifer management. Previous studies have shown that integration of flow pressure data can identify some large-scale trend of permeability variation in aquifer model, particularly the high-permeability channels, low-permeability barriers and variations near the wellbore areas (e.g. Wen, 1996; Capilla et al., 1997; Wen et al., 1998a,b).

In this paper, we extend the SSC technique to integrate transport data, namely, the tracer breakthrough

curves at pumping wells. A streamline-based tracer flow simulator (Batycky et al., 1997) is adapted for this purpose. A 1D analytical streamline solution is utilized for fast calculation of sensitivity coefficients of tracer breakthrough. The objective function to be minimized in the SSC method is in the form of

$$O = \sum_{t_p=1}^{n_{t,p}} \sum_{w=1}^{n_{w,p}} W_p(w_p, t_p)[\hat{p}(w_p, t_p) - p(w_p, t_p)]^2 + \sum_{t_f=1}^{n_{t,f}} \sum_{w_f=1}^{n_{w,f}} W_f(w_f, t_f)[\hat{f}(w_f, t_f) - f(w_f, t_f)]^2 \quad (1)$$

where $\hat{p}(w_p, t_p)$ and $p(w_p, t_p)$ are the observed and simulated pressure values at well w_p at time t_p. $\hat{f}(w_f, t_f)$ and $f(w_f, t_f)$ are the observed and simulated tracer breakthrough rates at well w_f at time t_f. W_p, and W_f are weights assigned to the pressure and tracer breakthrough data at different wells and at different times. $n_{w,p}$ and $n_{w,f}$ are the number of wells that have pressure and tracer breakthrough rate data. $n_{t,p}$ and $n_{t,f}$ are the number of time steps for the observed pressure and tracer breakthrough data, respectively.

A gradient method is used to minimize the above objective function, which requires the sensitivity coefficients (derivatives) of pressure, and breakthrough rate with respect to the permeability changes at the selected master locations. The method for computing sensitivity coefficients of pressure has been reported previously, i.e. they are obtained as part of the flow simulation run (Gomez-Hernandez et al., 1997; Wen et al., 1998a). The sensitivity coefficients of tracer breakthrough can be computed by a fast streamline-based method, i.e. they can be obtained by simply bookkeeping streamlines in the model by using the 1D analytical tracer movement solution along each streamline. The details of this method are given in Section 3.

In the current implementation, we assume that porosity is known and we are interested only in inverting for permeability field from dynamic flow and transport data. In addition, we assume that boundary conditions are known. We also assume that tracer is non-reactive and local dispersion is neglected in the tracer transport simulation.

In the following sections, we review the method for computing sensitivity coefficients of tracer breakthrough with the streamline-based method. This method is then implemented in the SSC inversion to construct aquifer permeability models. A synthetic example is used to demonstrate the efficiency of this approach and the robustness of the inverse results. The importance of integrating tracer data is illustrated by comparing the inverse results using different data sets to the true reference field. The accuracy and uncertainty of aquifer flow and transport predictions are compared.

3. Computation of sensitivity coefficients

Calculation of sensitivity coefficients takes the most computational effort in the SSC inversion. An efficient way of obtaining the sensitivity coefficient is essential for fast and feasible inversion. A streamline-based method for computing sensitivity coefficient of breakthrough data was proposed by Wen et al. (1998c). The sensitivity coefficients of tracer breakthrough at all master points can be obtained simultaneously by using the 1D analytical tracer solutions along the streamlines that define the flow field. The 1D analytical solution expresses the relationship between the tracer concentration and travel time along the streamline. The perturbations at all master locations are jointly considered in the sensitivity coefficient calculation. The key assumption is that streamline geometry is insensitive to the perturbation of the permeability field.

The tracer breakthrough rate (relative to the total flow rate) for a given pumping well w_f at time t_f can be expressed as (see Batycky et al., 1997)

$$f(w_f, t_f) = \frac{\sum_{l=1}^{n_{w_f}^{\mathrm{sl}}} q_l^{\mathrm{sl}} f_l^{\mathrm{sl}}(t_f)}{\sum_{l=1}^{n_{w_f}^{\mathrm{sl}}} q_l^{\mathrm{sl}}} \quad (2)$$

where q_l^{sl} is the flow rate associated with the streamline l, and $f_l^{\mathrm{sl}}(t_f)$ is the fractional flow rate (tracer concentration) of streamline l at time t_f. $n_{w_f}^{\mathrm{sl}}$ is the total number of streamlines arriving at the pumping well w_f. The derivative of $f(w_f, t_f)$ with respect to the

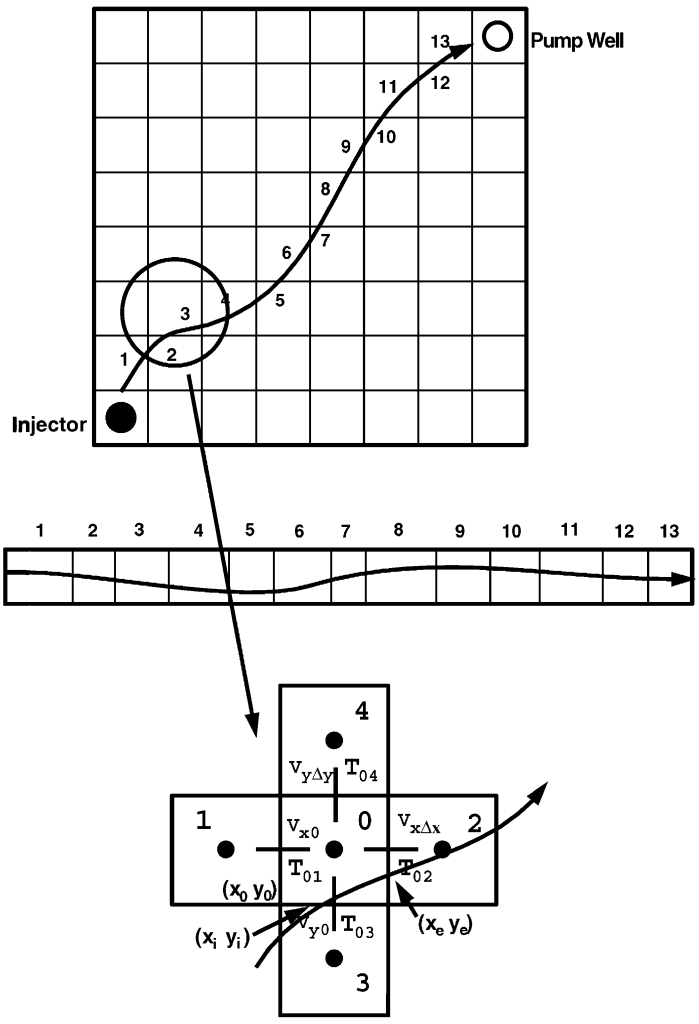

Fig. 2. Schematic illustration of tracking a streamline in a discretized numerical model.

permeability perturbation at master point j is then

$$\frac{\partial f(w_f,t_f)}{\partial k_j} = \frac{1}{\sum_{l=1}^{n_{w_f}^{sl}} q_l^{sl}} \sum_{l=1}^{n_{w_f}^{sl}} q_l^{sl} \frac{\partial f_l^{sl}(t_f)}{\partial k_j} \tag{3}$$

For non-reactive tracer flow without local dispersion, the tracer concentration along streamline l for a given time $f_l^{sl}(t_f)$ is the following function of travel time (τ_l) :

$$f_l^{sl}(t_f) = \begin{cases} 1 & \text{if } \tau_l \le t_f \\ 0 & \text{if } \tau_l > t_f \end{cases} \tag{4}$$

The travel time of a streamline is defined as

$$\tau_l = \int_0^l \frac{1}{v_l} \mathrm{d}r$$

with v_l being the pore velocity along the streamline l.

The $f_l^{sl}(t_f)$ in Eq. (4) is a step function. In order to compute the derivative of $f_l^{sl}(t_f)$, we can approximate it using an Error Function, i.e.

$$f_l^{sl}(t_f) \approx 1 - E\left(\frac{\tau_l}{t_f}\right)$$

and hence, we have

$$\frac{\partial f_l^{\mathrm{sl}}(t_f)}{\partial k_j} = -\frac{1}{t_f} G\left(\frac{\tau_l}{t_f}\right) \frac{\partial \tau_l}{\partial k_j} \tag{5}$$

with $G(\tau_l/t_f)$ being the Gaussian distribution function with mean 1 and a small variance. The computed sensitivity coefficients are shown to be quite stable with a variance in the range of 0.01–0.001 (Wen et al., 1998c). It should be noted that when considering local tracer dispersion, we could choose this variance to match the local longitudinal dispersion coefficient. We would also require an appropriate representation of local transverse dispersion within streamlines (see Blunt et al., 1996). This is outside the scope of this paper. Moreover, Smith and Schwartz (1980) have shown that field scale dispersion of mass transport is controlled essentially by the spatial variation of permeability in heterogeneous media. For the advection dominant transport problems, local dispersion can usually be neglected for field scale problems provided that the heterogeneity is described at sufficiently fine scale. This is consistent with the intention of the streamline simulation, where detailed aquifer descriptions are usually used.

The sensitivity coefficient of tracer breakthrough is then a function of the sensitivity coefficients of tracer travel time. In a numerical model, the travel time from an injection well to a pumping well is the sum of all travel times of all cells passed by this streamline:

$$\tau_l = \sum_{c=1}^{n_{l,c}} \Delta\tau_{l,c}$$

It can be shown that the sensitivity of travel time of streamline l to the permeability perturbation at master point j is the following (Wen et al., 1998c), see Fig. 2:

$$\frac{\partial \tau_l}{\partial k_j} = \sum_{c=1}^{n_{l,c}} \left\{ \sum_{g=1}^{4} \frac{\partial \Delta\tau_{l,c}}{\partial T_{0g}} \frac{\partial T_{0g}}{\partial k_j} + \sum_{m=0}^{4} \frac{\partial \Delta\tau_{l,c}}{\partial p_m} \frac{\partial p_m}{\partial k_j} \right\} \tag{6}$$

where $\Delta\tau_{l,c}$ is the travel time of streamline l crossing cell c. $n_{l,c}$ is the total number of cells that streamline l intersects from its starting point to its ending point. T_{0g}, $(g = 1, \ldots, 4)$, are the transmissivities for the four interfaces of cell 0 intersected by streamline l (see Fig. 2), p_m, $(m = 0, 1, \ldots, 4)$, are the pressure at the cell 0 and its surrounding cells. $(\partial\Delta\tau_{l,c})/(\partial T_{0g})$ and $(\partial\Delta\tau_{l,c})/(\partial p_m)$ can be computed from the semi-analytical expressions of travel time crossing a cell (see Pollock, 1989). $(\partial p_m)/(\partial k_j)$ is the sensitivity coefficient of pressure with respect to permeability change at master location j.

From Eq. (6), we see that the calculation of sensitivity coefficients is reduced to a simple bookkeeping of streamlines in the simulation model, which is both mathematically simple and computationally fast. The required sensitivity coefficients are obtained simultaneously within a single simulation run, and the spatial correlation of permeability perturbations at multiple master locations is accounted for through $(\partial T_{0g})/(\partial k_j)$. This method is faster and more accurate than the more traditional perturbation method (Wen et al., 1998c).

This method has been implemented in the SSC framework. A finite-difference method is used to solve the flow equations for the pressure field and sensitivity coefficients of pressure at all cells. Master points are randomly selected and their locations are changed after every 3–4 outer iterations. The flow equations are resolved and streamline geometry updated after every outer iteration, which 'self-corrects' the assumption of unchanging streamline geometry.

It is important to note that this method of computing sensitivity coefficients explicitly accounts for the effects of pressure on the travel time of a streamline. It requires the sensitivity coefficients of pressure in the entire model. An even simpler and faster way than Eq. (6) can be used to obtain the same sensitivity coefficients if we assume that the pressure gradient is insensitive to the permeability perturbations.

According to the travel time definition, the travel time that a streamline l needs to pass a given cell c is

$$\Delta\tau_{l,c} = \int_{l_{\mathrm{in}}}^{l_{\mathrm{out}}} \frac{1}{v_{l,c}} \mathrm{d}r = \int_{l_{\mathrm{in}}}^{l_{\mathrm{out}}} \frac{\phi_c \mu}{k_c |J|} \mathrm{d}r \tag{7}$$

where ϕ_c is the porosity at cell c, k_c is the permeability at cell c, μ is the fluid viscosity, and $|J|$ is the pressure gradient within cell c. Assume the pressure gradient is insensitive to the pressure changes due to the permeability perturbation, i.e. $|J|$ is constant, we have

$$\frac{\partial \Delta\tau_{l,c}}{\partial k_c} = -\frac{\Delta\tau_{l,c}}{k_c} \tag{8}$$

Thus, the sensitivity of travel time with respect to

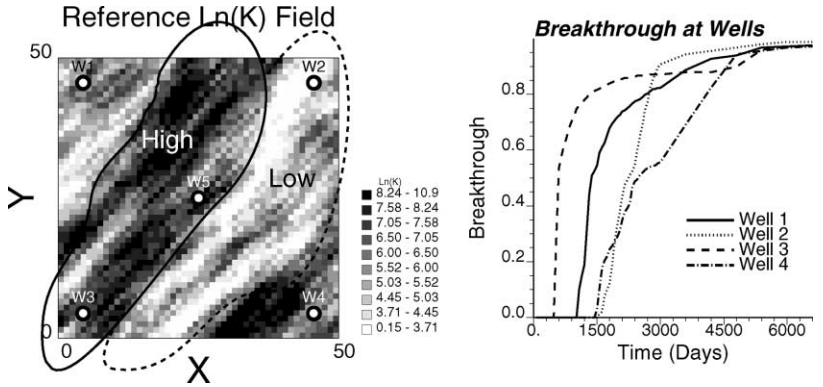

Fig. 3. A synthetic reference field and the tracer breakthrough curves from the four pumping wells.

the permeability at a given master location j can be computed as

$$\frac{\partial \Delta\tau_{l,c}}{\partial k_j} = \frac{\partial \Delta\tau_{l,c}}{\partial k_c}\frac{\partial k_c}{\partial k_j} = -\frac{\Delta\tau_{l,c}}{k_c}\varpi_{j,c} \tag{9}$$

where $\varpi_{j,c}$ is the kriging weight of master point j to cell c, which accounts for the correlation of k at the two locations. Thus, we have the required sensitivity coefficient of travel time as

$$\frac{\partial \tau_l}{\partial k_j} = \sum_{c=1}^{n_{slc}} \frac{\partial \Delta\tau_{l,c}}{\partial k_j} = \sum_{c=1}^{n_{l,c}} \frac{\partial \Delta\tau_{l,c}}{\partial k_c}\frac{\partial k_c}{\partial k_j}$$

$$= -\sum_{c=1}^{n_{l,c}} \left(\frac{\Delta\tau_{l,c}}{k_c}\varpi_{j,c}\right) \tag{10}$$

Based on this equation, we do not need to compute pressure sensitivity coefficients of the entire model for the computation of breakthrough sensitivity coefficients, which makes this method much faster. In most cases, the later method provides good enough results. A similar approach is used by Vasco et al. (1998).

4. Example

In this section, we demonstrate this streamline-based SSC inverse method for constructing aquifer permeability models from pressure and tracer transport data using a synthetic data set. We compare results inverted from different sets of dynamic data (pressure data only, tracer breakthrough data only, and both pressure and breakthrough data). In all cases, we assume porosity is known and constant at $\phi = 0.2$.

Fig. 3 shows a 2-D reference-data field (50×50 grid with cell size 80×80 m^2). The model was generated using sequential Gaussian simulation (SGSIM) (Deutsch and Journel, 1998). The $\ln(k)$ has a Gaussian histogram with mean and variance of 6.0 and 3.0, respectively. The unit of permeability (k) is millidarcy (1 darcy $= 9.8697 \times 10^{-13}$ m^2). The variogram is spherical with range of 800 and 160 m in the direction of 45 and 135°, respectively. Some general observations about this field are (1) a high permeability zone and a low permeability zone in the middle of the field, (2) high connectivity between well W5 and well W3, and (3) low connectivity between wells W5 and W2 and between wells W5 and W4. This reference field is considered as the true earth model, and our goal is to reconstruct aquifer models based on some flow and transport data that are close to this true field.

We assume that there is an injector at the center of the model with four pumping wells at the four corners. The injection rate at the central well (W5) is 1600 m^3/day, and the pumping rate for the four pumping wells (W1–W4) is 400 m^3/day/well. The thickness of the aquifer is assumed to be constant at 100 m. All four boundaries are assumed no-flow with initial pressure being constant at 3000 psi (1 psi = 6894.757 Pa) for the entire field. Flow is first solved using finite-difference method to obtain the transient pressure responses until it reaches steady state. Tracer transport is then solved using the streamline method by injecting tracer at the injection well continuously when flow is steady

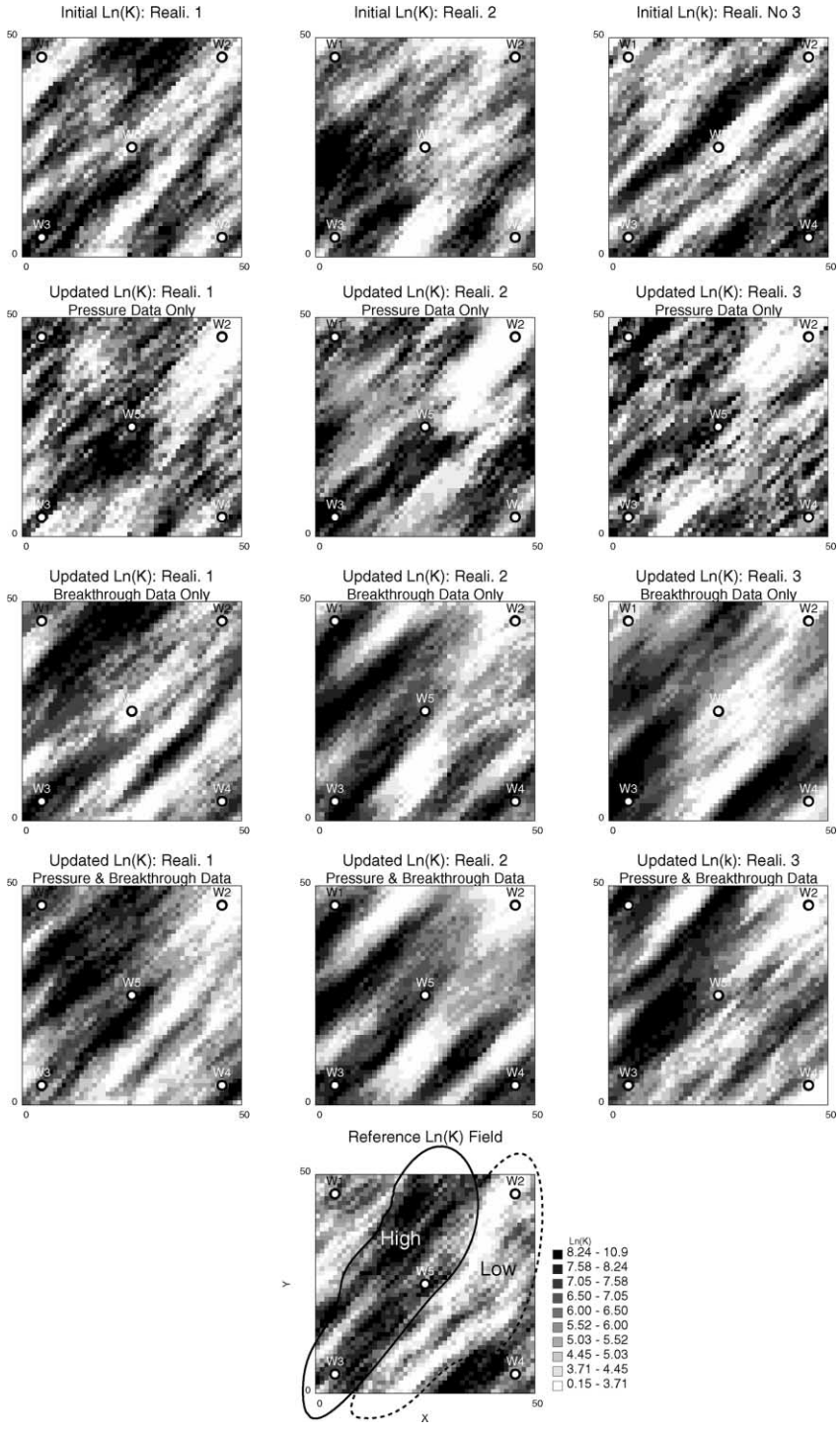

Fig. 4. Three realizations of initial models (top) and the SSC inverted models using different dynamic data sets. The reference field is displayed at the bottom.

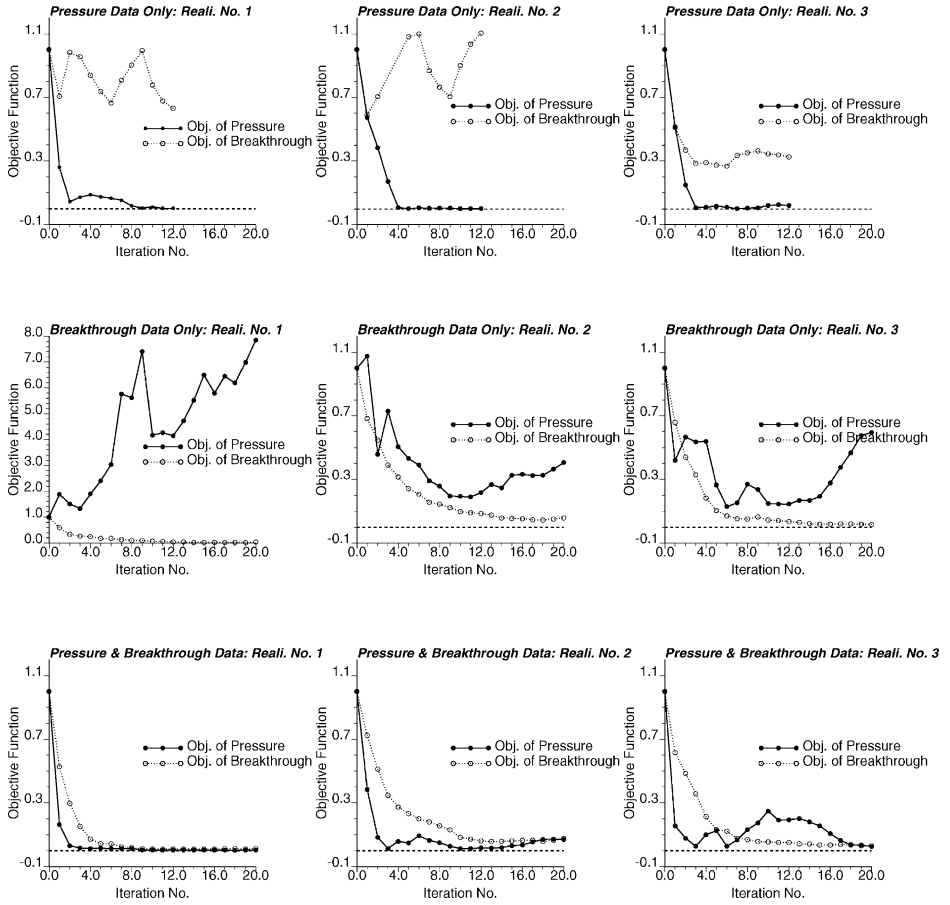

Fig. 5. Variations of the two components of objective function during the inversion iteration process in the three realizations when different dynamic data sets are used.

state. The tracer breakthrough curves at the four pumping wells are given in Fig. 3. The resulting transient pressure data (from initial to steady state) at the five wells and tracer breakthrough curves at the four pumping wells up to 1800 days are assumed to be the available dynamic data that will be used for inverting permeability model. All dynamic data used in the inversion are assumed precise without measurement error. It is noted that the problem setting and well configuration used in this example is to mimic the five well pattern configuration widely seen in the petroleum industry.

We first generate multiple initial realizations using the same histogram and variogram as the reference field. Neither well data nor other soft data is used to generate the initial models. We understand that some hard (e.g. core data) or soft (e.g. seismic data or borehole descriptions) data are usually available in practice. All relevant data should be used while constructing the initial models and these constraints can be preserved in the SSC inversion (see Wen et al., 1996; Capilla et al., 1998). For this example, we assume that these data are not available due to the practical consideration that the available data are usually at scales different from the cell size used in simulations.

Fig. 4 shows three initial permeability fields (top row) and the resulting fields updated by the SSC method using different data sets: only pressure at the five wells (second row), only breakthrough curves at the four pumping wells (third row), and both pressure and breakthrough data (fourth row). The reference

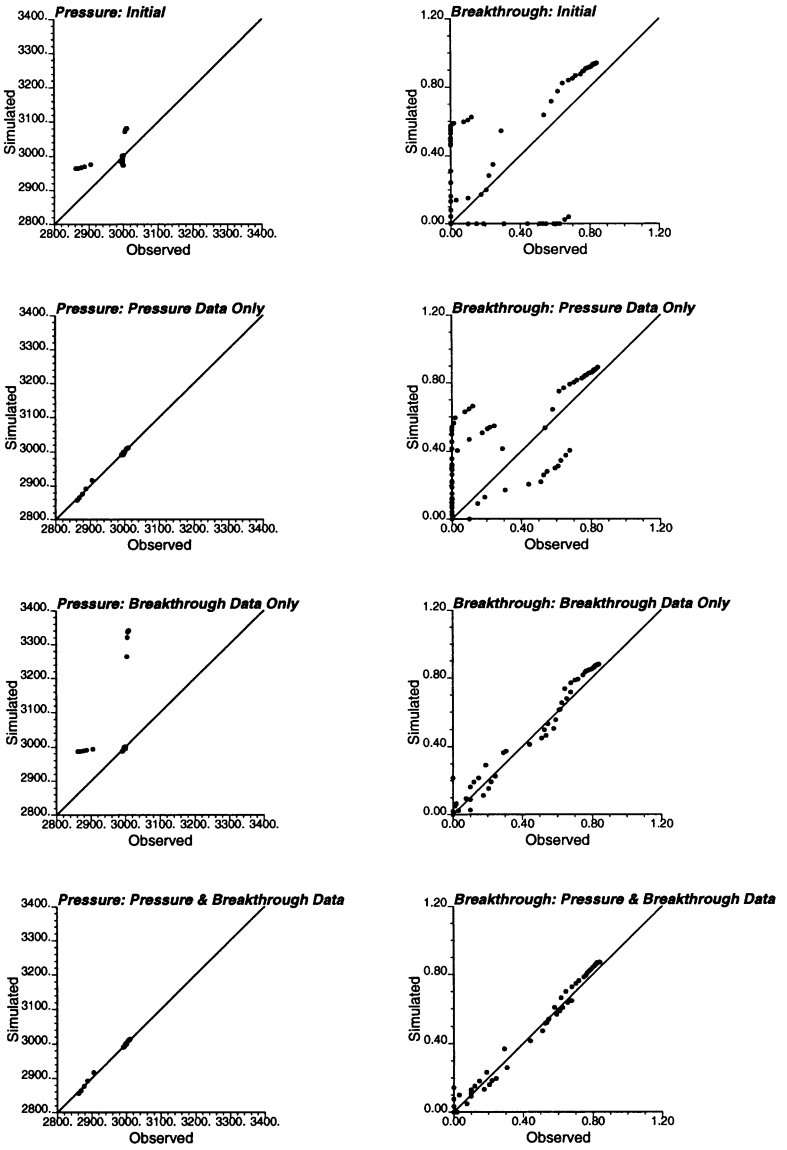

Fig. 6. Matching of pressure (left) and breakthrough (right) in one inverted permeability realization using different dynamic data sets.

field is given at the bottom for comparison. The changes in the two objective function components with the iteration number for the three realizations are given in Fig. 5. Twenty-five randomly selected master points are used for each realization. The variogram calculated from the exhaustive reference field is used for propagating the perturbations from the master locations to the entire field. The reference histogram is honored in all updated realizations through a post-process. Twenty SSC iterations are used for obtaining the final permeability models in all realizations. The CPU time for generating one realization is about 10 min (SGI Indigo workstation) for the case of matching both pressure and breakthrough data (i.e. the forth row in Fig. 4). Less CPU time is required when only matching pressure or breakthrough data alone.

From Fig. 4, we see qualitatively that the initial

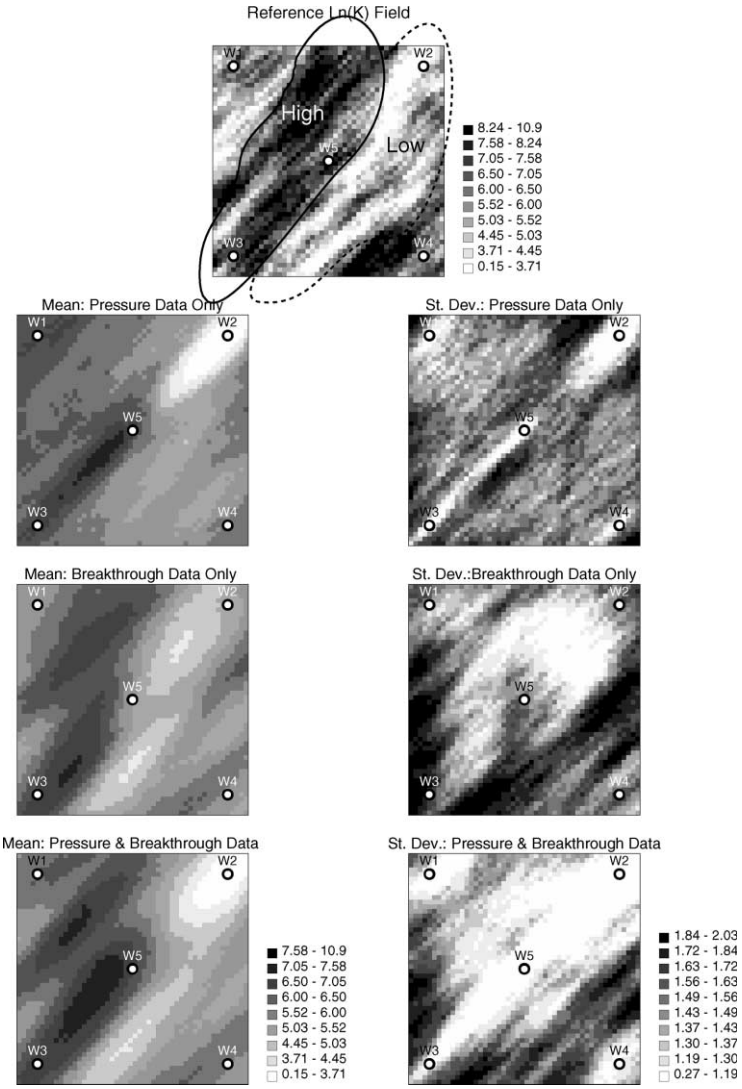

Fig. 7. Ensemble means (left) and standard deviations (right) from 200 permeability realizations inverted by using different sets of dynamic data. The reference field is displayed at the top.

permeability realizations (with only the correct variogram and histogram) poorly reproduce the reference field. As the initial models are updated by conditioning to dynamic data, the model representation improves. The closest results are those inverted by using both pressure and breakthrough data jointly (fourth row of Fig. 4). Fig. 5 gives a quantitative comparison of the objective function convergence for the updated models. The breakthrough data component of the objective function is not constrained when only pressure data are used to invert the permeability field (first row). Similarly, when only breakthrough data are used, the resulting permeability field may provide pressure responses, which deviate considerably from the true field (see the first realization in the second row of this figure). It is only when both pressure and breakthrough data are used that the resulting permeability models reproduce both pressure and breakthrough data jointly with both components of the objective function decreasing to close to zero (third row).

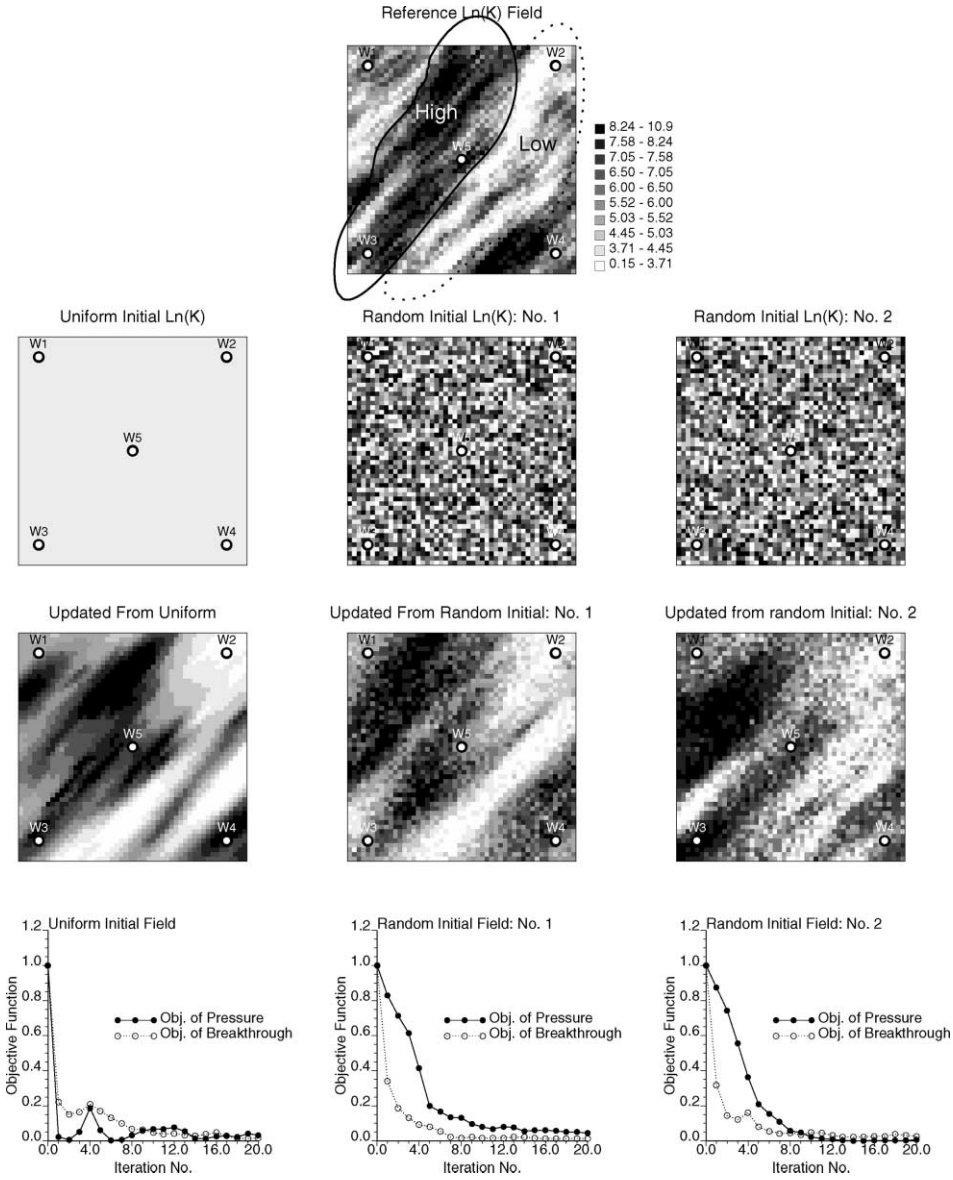

Fig. 8. The inverse results by using uniform and pure random fields as initial models. The variations of objective function are displayed at the bottom.

The comparisons of simulated and observed pressure and breakthrough data for the first realization are given in Fig. 6. We see that both pressure and breakthrough data deviate considerably from the true results in the initial fields (first row). Pressure data are exactly matched when only pressure data are used to match, but breakthrough data largely deviate from the data (second row). When only breakthrough data are used, the model reproduces the breakthrough data but not for the pressure data (third row). Both pressure and breakthrough data are accurately matched when both data sets are used to constrain the model (fourth row).

A better comparison of the inverse results using

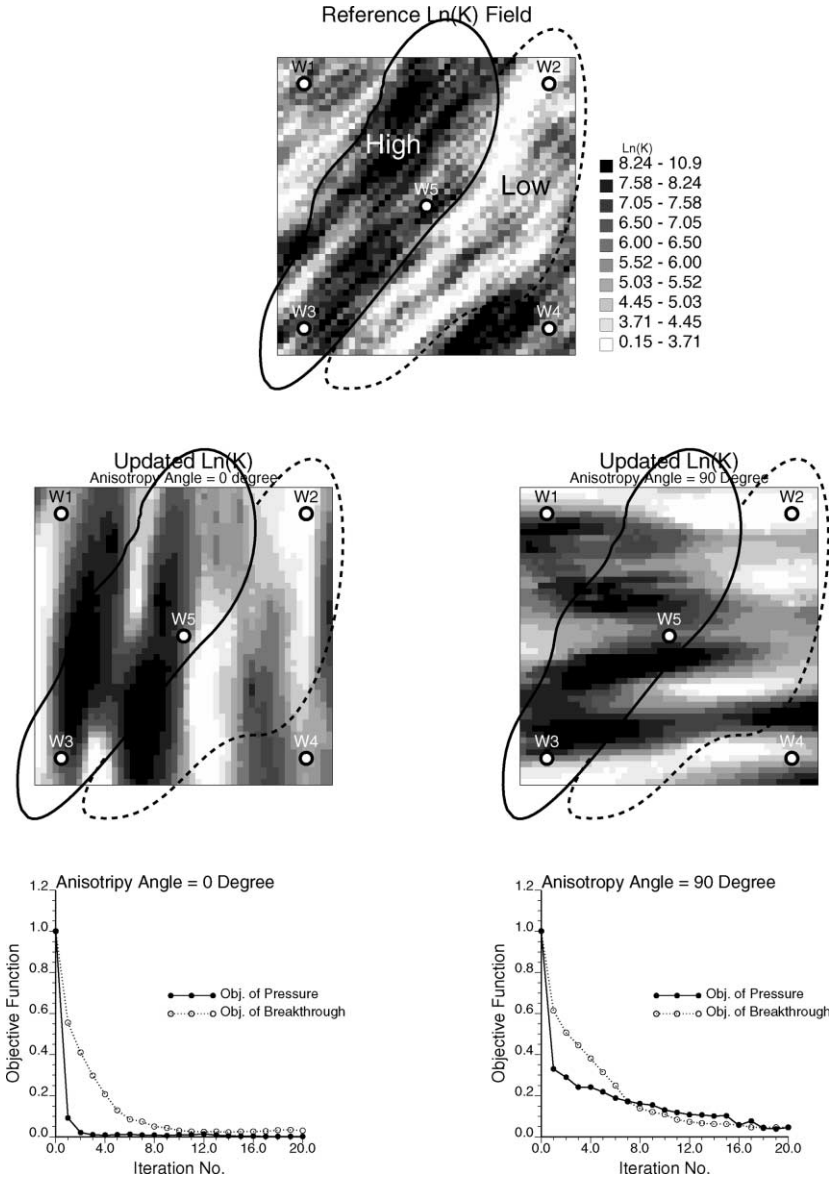

Fig. 9. The inversion results using wrong variogram models. The variations of objective function are displayed at the bottom.

the different data sets is given by the ensemble results calculated from 200 realizations (Fig. 7). The ensemble mean field represents the common trend in the multiple realizations, while the standard deviation field displays the variations (or uncertainty) among the realizations. For the initial fields, no additional spatial information is retained except the mean (6.0) and variance (3.0) everywhere in the ensemble fields. Some large-scale spatial patterns can be identified from the pressure data alone with reduced uncertainty in the areas near to the well locations only (second row). More spatial variation patterns are identified from the breakthrough data with reduced uncertainty in the inter-well areas (third row). The best results are those when both pressure and breakthrough data are

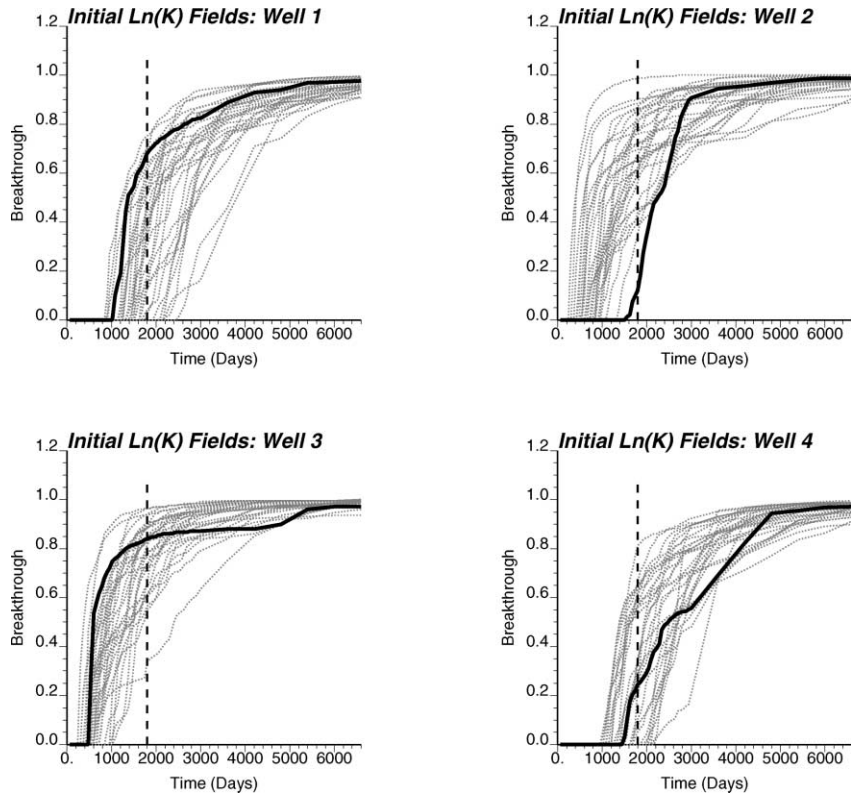

Fig. 10. Predictions of tracer breakthrough at the four pumping wells from the 30 initial realizations. Thick lines are the reference results.

used (bottom row): they accurately reproduce most of the spatial variation features in the reference field with much less uncertainty, as compared to the results using only pressure or breakthrough data alone.

To test the robustness of the inverse algorithm with different initial models, we start from initial models with completely wrong features relative to the reference field. These wrong models are then updated to match the pressure and breakthrough data. We also investigate the influence of inverse results by using wrong variogram models since variogram model may be uncertain in practice.

Fig. 8 shows the results updated from a uniform permeability field and two purely random permeability fields. The changes of the two objective function components are also given at the bottom row of this figure. The three final updated models (after 20 SSC iterations) reproduce the spatial variation patterns of the reference field (shown at the top). The model updated from the uniform initial model displays smoother variations than the true field, while the models updated from the purely random initial fields display more fuzzy small-scale feature with correct large-scale patterns. All updated models accurately match both the pressure and breakthrough data with objective functions close to zero.

Fig. 9 shows the inverse results updated from a uniform initial field by using incorrect variogram models: one with the major correlation in *Y*-direction, and the other with the major correlation in *X*-direction. The final results, although different in appearance from the reference field, still correctly identify the relative locations of high and low permeability regions, as well as the spatial connections between well pairs. Both pressure and breakthrough data are accurately reproduced in both models as well. From above, we can conclude that the SSC method is quite robust.

As mentioned before, we only use breakthrough

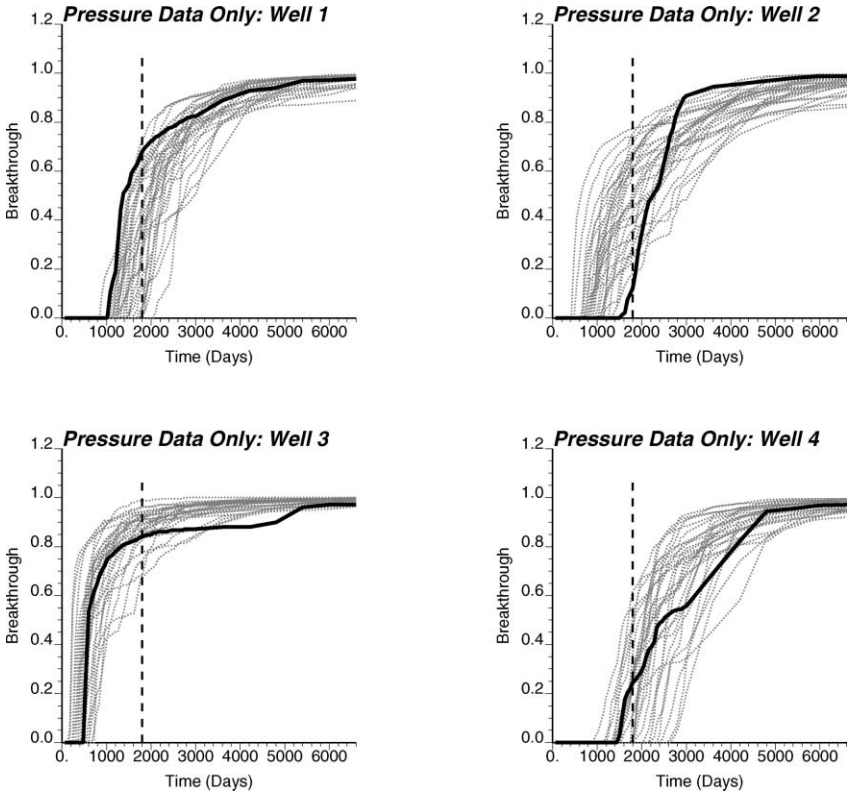

Fig. 11. Predictions of tracer breakthrough at the four pumping wells from the 30 SSC inverted realizations using pressure data alone. Thick lines are the reference results.

data up to 1800 days in the inversion. Now, we investigate the importance of integrating different flow and transport data for future predictions of tracer transport in the aquifer. We compare the quality of predictions of tracer breakthrough at the four pumping wells from 1800 to 6600 days with the same well conditions (i.e. the same injection and pumping rate as used to match the models) using different permeability models. Using the initial fields where neither pressure data nor breakthrough data are matched, the breakthrough curves from 30 realizations are shown in Fig. 10: these predictions are neither accurate (deviate from the true results) nor precise (large uncertainty). When the pressure data at all the five wells are matched, the predictions in the four pumping wells from the 30 realizations are given in Fig. 11. Clear improvement is evident compared to the initial fields. However, these predictions are still not accurate with large uncertainty. This indicates that matching pressure data may not be sufficient for reliable predictions of tracer transport: more information is required. When the permeability models match only the early breakthrough data of 1800 days at the four pumping wells, the predictions are shown in Fig. 12. It is clear that the predictions of breakthrough at the four pumping wells are dramatically improved since the same type of early-time data at the same wells are matched. The best predictions are obtained by using the aquifer models in which both pressure and (early-time) breakthrough data at the same wells are conditioned, see Fig. 13.

5. Summary

The SSC method was used to generate multiple

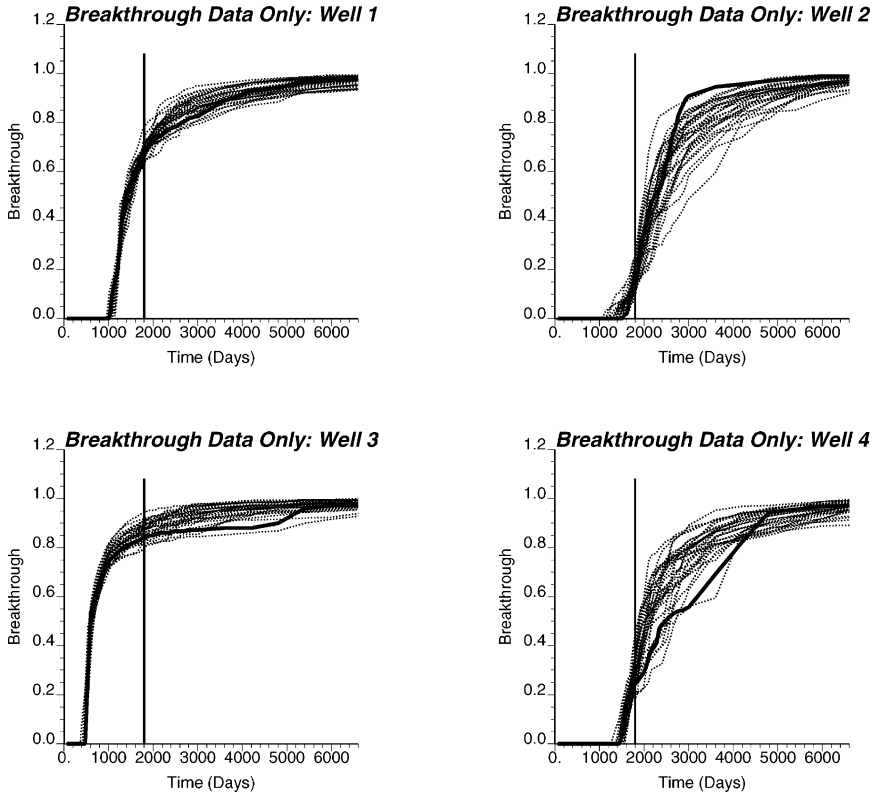

Fig. 12. Predictions of tracer breakthrough the four pumping wells from the 30 SSC inverted realizations using breakthrough data alone. Thick lines are the reference results.

realizations of aquifer permeability with the correct geostatistical features that match measured pressure data and tracer transport (breakthrough) data. An efficient streamline-based methodology was implemented for computing sensitivity coefficients of tracer breakthrough. This new method adapts the concept of decoupling multiple-dimensional transport problem into multiple 1D problems along streamlines. Using the analytical 1D solution along the streamline, the completed set of sensitivity coefficients is obtained simultaneously by bookkeeping all streamlines with only one simulation run. Moreover, the perturbations at all master locations are jointly considered through Kriging.

Application of the SSC method was demonstrated using a synthetic example, which shows the computational efficiency and robustness of the enhanced SSC method. Comparisons were made with different sets of dynamic data: pressure data only, breakthrough data only, and both pressure and breakthrough data. Aquifer performances are predicted using different models inverted from different dynamic data sets.

Results show that dynamic flow and transport data carry important information on the spatial variation of aquifer properties. Integration of more data ensures that spatial variation patterns are identified with less uncertainty. Pressure data carry information around the wells, tracer breakthrough data provide additional information on the spatial connectivity between the wells. Matching pressure or breakthrough data alone may still result in high uncertainty. Integrating pressure and breakthrough data jointly significantly improves the aquifer heterogeneity representation and aquifer performance predictions.

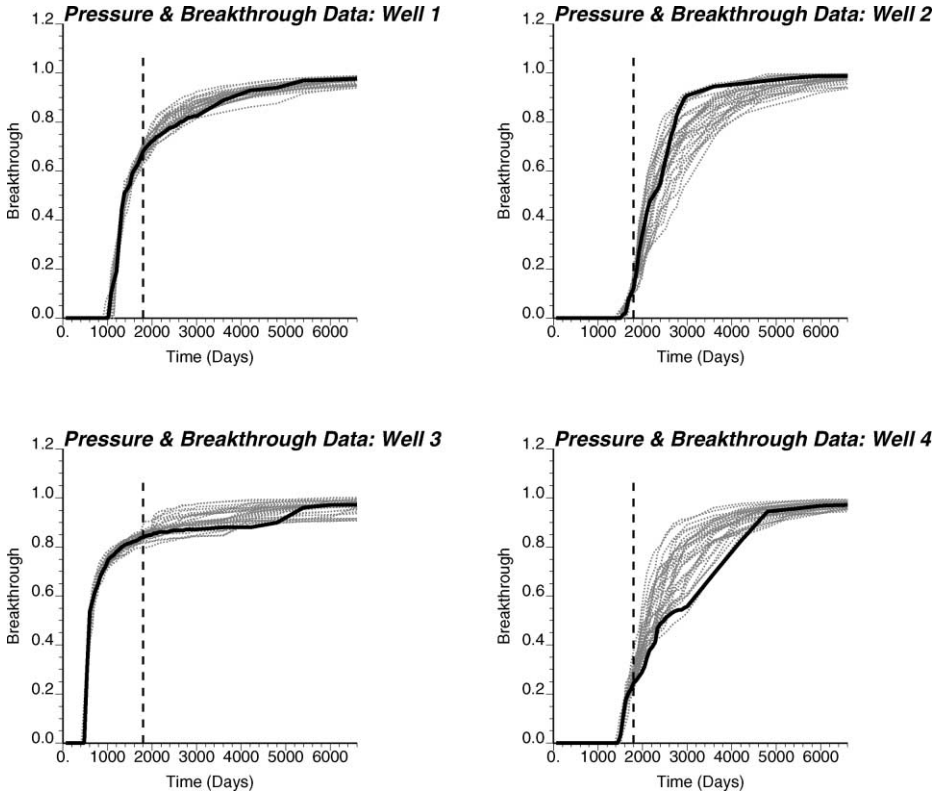

Fig. 13. Predictions of tracer breakthrough at the four pumping wells from the 30 SSC inverted realizations using both pressure and breakthrough data. Thick lines are the reference results.

Acknowledgements

We thank Prof. J.J. Gomez-Hernandez and Prof. J.E. Capilla at Technical University of Valencia, Spain for their support and assistance in developing the SSC extension. We also thank Prof. A.G. Journel of Stanford University for stimulating discussions and Mobil Petroleum Technology Company for partial support.

References

Batycky, R.P., Blunt, M.J., Thiele, M.R., 1997. A 3D field-scale streamline-based reservoir simulator. SPE Reservoir Engineering November, 246–254.

Blunt, M.J., Liu, K., Thiele, M.R., 1996. A generalized streamline method to predict reservoir flow. Petroleum Geosciences 2, 256–269.

Capilla, J.E., Gomez-Hernandez, J.J., Sahuquillo, A., 1997. Stochastic simulation of transmissivity fields conditional to both transmissivity and piezometric data. 2. Demonstration on a synthetic case. Journal of Hydrology 203 (1–4), 175–188.

Capilla, J.E., Rodrigo, J., Gomez-Hernandez, J.J., 1998. Geological structure of simulated transmissivity fields that honor piezometric data. Paper Presented at the Second European Conference on Geostatistics for Environmental Applications, 18–20 November, 1998, Valencia, Spain.

Carrera, J., Neuman, S.P., 1986. Estimation of aquifer parameter under transient and steady conditions: 3. Application to synthetic and field data. Water Resources Research 22 (2), 228–242.

Deutsch, C.V., Journel, A.G., 1998. GSLIB: Geostatistical Software Library and User's Guide. . 2nd edOxford University Press, New York 369 pp.

Gomez-Hernandez, J.J., Sahuquillo, A., Capilla, J.E., 1997. Stochastic simulation of transmissivity fields conditional to both transmissivity and piezometric data. 1. The theory. Journal of Hydrology 203 (1–4), 162–174.

Harvey, C.F., Gorelick, S.M., 1995. Mapping hydraulic conductivity: sequential conditioning with measurements of solute arrival time, hydraulic head, and local conductivity. Water Resources Research 31 (7), 1615–1626.

Kitanidis, P.K., 1996. On the geostatistical approach to the

groundwater inverse problem. Advanced Water Resources 19 (6), 333–342.

Pollock, D.W., 1989. Documentation of computer programs to compute and display pathline results from the US geological survey modular three-dimensional finite-difference groundwater flow model. Technical Report Open File Report 89-381, US Geological Survey.

RamaRao, B.S., LaVenue, A.M., de Marsily, G., Marietta, M.G., 1995. Pilot point methodology for automated calibration of an ensemble of conditionally simulated transmissivity fields. 1. Theory and computational experiments. Water Resources Research 31 (3), 475–493.

Smith, L., Schwartz, F.W., 1980. Mass transport. 1. A stochastic analysis of macroscopic dispersion. Water Resources Research 17 (5), 1463–1479.

Sun, N.-Z., 1994. Inverse Problem In Groundwater Modeling. Kluwer Academic Publishers, Boston 337 pp.

Tarantola, H., 1987. Inverse Problem Theory: Methods for Data Fitting and Model Parameter Estimation. Elsevier, Amsterdam 613 pp.

Vasco, D.W., Yoon, S., Datta-Gupta, A., 1998. Integrating dynamic data into high-resolution reservoir models using streamline-based analytical sensitivity coefficients. SPE paper 49002 presented at the 1998 SPE Annual Technical Conference and Exhibition, New Orleans, LA, 27–30 September.

Wen, X.-H., 1996. Stochastic simulation of groundwater flow and mass transport in heterogeneous aquifers: conditioning and problem of scales. PhD Dissertation. Polytechnic University of Valencia, Valencia, Spain, 260 pp.

Wen, X.-H., Gomze-Hernandez, J.J., Capilla, J.E., Sahuquillo, A., 1996. The significance of conditioning on piezometric head data for predictions of mass transport in groundwater modeling. Mathematical Geology 28 (7), 961–968.

Wen, X.-H., Deutsch, C.V., Cullick, A.S., 1997. A review of current approaches to integrate flow production data in geological modeling. Report 10, Stanford Center for Reservoir Forecasting, Stanford, CA.

Wen, X.-H., Deutsch, C.V., Cullick, A.S., 1998a. High resolution reservoir models integrating multiple-well production data. SPE Journal December, 344–355.

Wen, X.-H., Deutsch, C.V., Cullick, A.S., 1998b. Integrating pressure and fractional flow data in reservoir modeling with fast streamline-based inverse method. SPE paper number 48971.

Wen, X.-H., Deutsch, C.V., Cullick, A.S., 1998c. A fast streamline-based methsod for computing sensitivity coefficients of fractional flow rate. SPE Journal, submitted for publication.

Wen, X.-H., Capilla, J.E., Deutsch, C.V., Gomez-Hernandez, J.J., Cullick, A.S., 1999. A program to create permeability fields that honor single-phase flow rate and pressure data. Computers and Geosciences 25, 217–230.

Yeh, W.W.-G., 1986. Review of parameter identification procedure in groundwater hydrology: the inverse problem. Water Resources Research 22 (2), 85–92.

Yeh, T.-C., Jin, M., Hanna, S., 1996. An iterative stochastic inverse method: conditional effective transmissivity and hydraulic head fields. Water Resources Research 32 (1), 85–92.

Zimmerman, D.A., Axness, C.L., de Marsily, G., Marietta, M.G., Gotway, C.A., 1995. Some results from a comparison study of geostatistically-based inverse techniques. Sandia National Laboratories, Albuquerque, NM, USA.